

Quantum Location Verification in Noisy Channels

Robert A. Malaney, School of Electrical Engineering and Telecommunications, University of New South Wales, NSW 2052, Australia. r.malaney@unsw.edu.au

Abstract—Recently it has been shown how the use of quantum entanglement can lead to the creation of real-time communication channels whose viability can be made location dependent. Such functionality leads to new security paradigms that are not possible in classical communication networks. Key to these new security paradigms are quantum protocols that can unconditionally determine that a receiver is in fact at an *a priori* assigned location. A limiting factor of such quantum protocols will be the decoherence of states held in quantum memory. Here we investigate the performance of quantum location verification protocols under decoherence effects. More specifically, we address the issue of how decoherence impacts the verification using $N = 2$ qubits entangled as Bell states, as compared to $N > 2$ qubits entangled as GHZ states. We study the original quantum location verification protocol, as well as a variant protocol, introduced here, which utilizes teleportation. We find that the performance of quantum location verification is in fact similar for Bell states and some $N > 2$ GHZ states, even though quantum decoherence degrades larger-qubit entanglements faster. Our results are important for the design and implementation of location-dependent communications in emerging quantum networks.

I. INTRODUCTION

The ability to offer a real-time communication channel whose viability is unconditionally a function of the receiver location would offer a range of new information security paradigms and applications (*e.g.* see discussions in [1], [2], [3], [4]). The ability to guarantee location-sensitive communications requires unconditional (independent of the physical resources held by an adversary) location verification. However, given that an adversary can possess unlimited receivers, each of which can be presumed to possess unlimited computational capacity, it is straightforward to see why classical-only unconditional location verification is impossible. Classical location verification use ‘challenges’, and the finite speed of light, in order to bound ranges. As such, an adversary with multiple receivers can simply delay the response to a challenge in order to circumvent verification (see discussion in [2], [4] for more detail on verification limits of classical systems). However, recently it has been shown how the introduction of quantum entanglement into the communication channel leads to an unconditional *quantum location verification* (QLV) protocol [5]. In [5] quantum entanglement is used to develop a ‘cloaked’, and distributed, superdense coding system, in which the response times to (classical) challenges are measured in order to provide location verification. In QLV the answer to a classical challenge is encoded in entangled quantum states. Due to the fact that quantum information cannot be perfectly copied [6], only a device containing all qubits of the entangled state can decode successfully, and only a device at a specified location can answer within the required timescale. For a more detailed description of QLV the reader is referred to [5]. For

more details on superdense coding, including experimental status, the reader is referred to [7], [8]. Details relating to some recent experiments involving entanglement, including its use in quantum teleportation [9], can be found in [10], [11]. Discussion of the largest quantum communications network yet built can be found in [12].

In [5] QLV was explored under the assumption of perfect quantum channels. More specifically, it was assumed that the principal resource of QLV, the entanglement between qubits, was preserved perfectly. In any practical system of course this will not be true. This is especially the case since quantum memory is required for the most useful variants of the QLV protocol. The current experimental status regarding quantum memory is reviewed in [13] (see also [14]), where we learn that current timescales for successful storage of multipartite entangled states is in the order of milliseconds. Heroic efforts to increase such storage times to that required for workable large-scale quantum networks (*i.e.* seconds) is currently underway in many laboratories [13]. The limiting factor in quantum memory is decoherence effects, where qubit-environment interactions destroy the fragile entanglement of the quantum states. It is the purpose of this work to explore the effect quantum decoherence has on the performance of QLV. We will be specifically interested in the impact of decoherence on two-qubit maximally entangled states, relative to three-qubit (and higher) maximally entangled states. As described more below, QLV protocols use two-qubit and larger-qubit entangled states in a different manner.

II. DECOHERENCE IN QLV

A. Bell States and GHZ States in QLV

Consider some system state $|\Psi_s\rangle$, which we can use as a means of encoding and decoding a secret sequence of bits. In the QLV protocol of [5] location verification of a device can be obtained by setting $|\Psi_s\rangle$ to the Bell states. If N is the number of qubits entangled, the four orthogonal basis states for a Bell state ($N = 2$) can be written,

$$|\Psi_s^{Bell}\rangle = \frac{1}{\sqrt{2}}(|00\rangle \pm |11\rangle), \frac{1}{\sqrt{2}}(|10\rangle \pm |01\rangle).$$

Alternatively, Green-Horne-Zeilinger (GHZ) [15] states in which $N = 3$ qubits are maximally entangled could be utilized. The eight orthogonal basis states of a $N = 3$ GHZ state can be written,

$$|\Psi_s^{GHZ}\rangle_{N=3} = \left\{ \frac{1}{\sqrt{2}}(|000\rangle \pm |111\rangle), \frac{1}{\sqrt{2}}(|001\rangle \pm |110\rangle) \right\}.$$

Larger qubit GHZ states are also available. For example, a basis state of N entangled qubits would be $|\Psi_s^{GHZ}\rangle_N =$

$\frac{1}{\sqrt{2}}(|000\dots N\rangle + |111\dots N\rangle)$ where the notation $|000\dots N\rangle = |0\rangle^{\otimes N}$ is the tensor product of the state $|0\rangle$, N times.¹ Henceforth, a state of the form $\frac{1}{\sqrt{2}}(|000\dots N\rangle + |111\dots N\rangle)$ is referred to as a ‘cat’ state.

In two dimensional location verification, at least three reference stations are required. With three reference stations, two Bell states would be required for each *instance of location verification*. Such an instance occurs every time the minimal amount of decoded information required for an independent location verification becomes available (e.g. steps 4-6 of the protocol detailed later represent one such instance). The qubits of the two Bell states required for each instance of location verification would be distributed between the three reference stations (a single qubit at two of the stations, and two qubits at a third station). However, using GHZ states, only one $|\Psi_s^{GHZ}\rangle_{N=3}$ state is required for the same instance of location verification. The three qubits of this state would also be distributed between the three reference stations (one qubit at each station).

For the protocol of [5], if the number of reference stations was also equal to N , then $\lceil N/2 \rceil$ Bell states² will be required for each instance of location verification, as opposed to one N -qubit GHZ state. The question we now address is the following. What is the performance of a QLV protocol with N reference stations, determined using $\lceil N/2 \rceil$ Bell states, relative to the performance based on a single maximally entangled GHZ state comprising N qubits? This question has important ramifications for the design of QLV protocols in emerging large-scale quantum networks.

B. Decoherence Models

A decoherence model is built by studying the time evolution of some initial system state $|\Psi_s\rangle$, as it interacts with some external environment whose initial state we write as $|\Psi_e\rangle$. Without loss of generality we will assume $|\Psi_s\rangle$ and $|\Psi_e\rangle$ are initially not entangled with each other.

In terms of the density operators $\rho_s = |\Psi_s\rangle\langle\Psi_s|$ and $\rho_e = |\Psi_e\rangle\langle\Psi_e|$, the initial state of the combined total system can be written as $\rho_s \otimes \rho_e$. Although the open evolution of the system ρ_s is described by a non-unitary evolution, the closed evolution of $\rho_s \otimes \rho_e$ can be described by a unitary U via $U(\rho_s \otimes \rho_e)U^\dagger$. To obtain the output system state, ρ_s^{out} , after some closed evolution U , we use $\rho_s^{out} \equiv \varepsilon(\rho_s) = \text{Tr}_e[U(\rho_s \otimes \rho_e)U^\dagger]$ where Tr_e is the partial trace over the environment’s qubits. The channel $\rho_s^{out} \equiv \varepsilon(\rho_s)$ is a completely positive, trace preserving, map which provides the required evolution of ρ_s . It is possible to describe such maps directly using an operator-sum representation,

$$\varepsilon(\rho_s) = \sum_{a=1}^M K_a \rho_s K_a^\dagger, \quad \text{where} \quad \sum_{a=1}^M K_a^\dagger K_a = I, \quad (1)$$

and where $K_{a=1\dots M}$ represent the so-called Kraus operators, with M being the number of operators [17]. One can show

¹Creation of GHZ states is reviewed in [16], where a ten-qubit *hyper-entangled* state is also demonstrated. A QLV protocol based on hyper-entanglement would be an extension of the protocol presented in [5].

² $\lceil x \rceil$ is the ceiling of x .

that a map given by Eq. (1) leads to affine transformations in the Bloch sphere coordinates of the state $|\Psi_s\rangle$ whose most general description requires 12 parameters. However, although a general model of decoherence for a single qubit requires these 12 parameters, it is important to note that these parameters cannot be arbitrarily chosen due to the constraint of complete positivity (any map given by Eq. (1) is automatically completely positive). As we discuss more below, there are special-case quantum channels where only a few parameters are needed in order to map the decoherence of a qubit.

Given a set of Kraus operators for a quantum channel, it is straightforward to calculate the probability that, in some post-decoherence measurement, the state ρ_s is recovered. This probability, which we refer to as the fidelity F , is given by

$$F = \text{Tr}(\rho_s \rho_s^{out}) = \text{Tr} \left(\rho_s \sum_{a=1}^M K_a \rho_s K_a^\dagger \right). \quad (2)$$

Note that F as defined here is the square of the normal fidelity described by $\text{Tr} \sqrt{(\rho_s^{1/2} \rho_s^{out} \rho_s^{1/2})}$. Clearly, a critical step is the determination of the appropriate Kraus operators for a given channel. As we are interested in probing QLV performance in the general case we will, in the first instance, construct the Kraus operators for the single qubits using random unitary matrices U_a . It is straightforward to show that given a set $\{U_a\}$, and a set of real non-negative numbers $\{p_a\}$ such that $\sum_a p_a = 1$, one can construct a set of Kraus operators $\{K_a\}$ where $K_a = \sqrt{p_a} U_a$ (e.g. [18]). For a single qubit there can be at most four ($a = 1\dots 4$) independent Kraus operators. Here we will construct four Kraus operators for a single qubit, by taking U_2, U_3 and U_4 to be random 2 dimensional unitaries. The first Kraus operator is set to the identity matrix ($U_1 = I_2$). In addition, the probability p_1 associated with U_1 will be set equal to the decoherence parameter, p , where $p = 1 - e^{-\gamma t}$, and where t is the time spent in the channel and γ is a rate associated with decoherence. By constraining the sets $\{p_a\}$ and $\{U_a\}$, it is possible to construct many different noisy channels. Although, in general, not mapping to any specific model of the qubit-environment interaction, the quantum channels just described, which we henceforth refer to as a *random noise channels*, will allow us to investigate in a generic manner the *relative* decoherence between the $N = 2$ (bipartite) Bell states and the $N > 2$ (multipartite) GHZ entangled states. We ignore in this work, the (in-principle) possibility of reversing decoherence in random noise channels using classical information extracted from the environment [19].

There are also decoherence channels modeled on specific qubit-environment interactions (e.g. see [20]). For example, consider the depolarization channel. Using the following relations for the Pauli matrices in the single-qubit basis; $\sigma_o = |0\rangle\langle 0| + |1\rangle\langle 1|$, $\sigma_x = |0\rangle\langle 1| + |1\rangle\langle 0|$, $\sigma_y = i(|1\rangle\langle 0| - |0\rangle\langle 1|)$, and $\sigma_z = |0\rangle\langle 0| - |1\rangle\langle 1|$; we can write the density operator for the $|\Psi_s^{GHZ}\rangle_N$ cat state as,

$$\rho_s^{GHZ}(N) = \frac{1}{2^{N+1}} \left(\begin{aligned} &(\sigma_o + \sigma_z)^{\otimes N} + (\sigma_o - \sigma_z)^{\otimes N} \\ &+ (\sigma_x + i\sigma_y)^{\otimes N} + (\sigma_x - i\sigma_y)^{\otimes N} \end{aligned} \right). \quad (3)$$

We again introduce the decoherence parameter, p , of a qubit where $0 \leq p \leq 1$, with $p = 1$ meaning complete decoherence and $p = 0$ meaning no decoherence. The depolarization channel for a single qubit can be defined as $\varepsilon(\rho_s) = (1-p)\rho_s + p\frac{\sigma_o}{2}$. Using the relation

$$\sigma_o = \frac{1}{2} \left(\rho_s + \sum_{j=1}^3 \sigma_j \rho_s \sigma_j \right),$$

we see that the Kraus operators for the depolarization channel can be written $K_1 = \sqrt{1 - \frac{3p}{4}}\sigma_o$, $K_2 = \sqrt{\frac{p}{4}}\sigma_x$, $K_3 = \sqrt{\frac{p}{4}}\sigma_y$, and $K_4 = \sqrt{\frac{p}{4}}\sigma_z$. Writing explicitly in terms of the Pauli matrices, and adopting time dependence $p = 1 - e^{-\gamma t}$ we have the following model for a N -qubit GHZ state undergoing decoherence in the depolarization channel, $\varepsilon_D(\rho_s^{GHZ})$

$$= \frac{1}{2^{N+1}} \left(\begin{array}{l} (\sigma_o + e^{-\gamma t}\sigma_z)^{\otimes N} + (\sigma_o - e^{-\gamma t}\sigma_z)^{\otimes N} \\ + e^{-N\gamma t} [(\sigma_x + i\sigma_y)^{\otimes N} + (\sigma_x - i\sigma_y)^{\otimes N}] \end{array} \right). \quad (4)$$

Here (and in all our models) we have assumed that in multi-qubit systems each qubit evolves in an equal and independent manner.

Similarly, we can describe the amplitude damping channel as

$$\varepsilon_{AD}(\rho_s) = \left(\begin{array}{cc} a + pc & (\sqrt{1-p})b \\ (\sqrt{1-p})b^* & (1-p)c \end{array} \right),$$

where we have used $\rho_s = \begin{bmatrix} a & b \\ b^* & c \end{bmatrix}$. This leads to two Kraus operators of the form $K_1 = \begin{bmatrix} 1 & 0 \\ 0 & \sqrt{1-p} \end{bmatrix}$ and $K_2 = \begin{bmatrix} 0 & \sqrt{p} \\ 0 & 0 \end{bmatrix}$. This, in turn, leads to an amplitude damping channel explicitly given as $\varepsilon_{AD}(\rho_s^{GHZ})$

$$= \frac{1}{2^{N+1}} \left(\begin{array}{l} (\sigma_o + \sigma_z)^{\otimes N} + (\sigma_o + (1 - 2e^{-\gamma t})\sigma_z)^{\otimes N} \\ + e^{-\frac{N\gamma t}{2}} [(\sigma_x + i\sigma_y)^{\otimes N} + (\sigma_x - i\sigma_y)^{\otimes N}] \end{array} \right). \quad (5)$$

A third commonly used channel is the phase damping channel which can be described by

$$\varepsilon_{PD}(\rho_s) = \left(\begin{array}{cc} a & (1-p)b \\ (1-p)b^* & c \end{array} \right),$$

leading to Kraus operators $K_1 = \begin{pmatrix} \sqrt{1-p} & 0 \\ 0 & \sqrt{1-p} \end{pmatrix}$, $K_2 = \begin{pmatrix} \sqrt{p} & 0 \\ 0 & 0 \end{pmatrix}$, and $K_3 = \begin{pmatrix} 0 & 0 \\ 0 & \sqrt{p} \end{pmatrix}$. This leads to a phase damping channel explicitly given as $\varepsilon_{PD}(\rho_s^{GHZ})$

$$= \frac{1}{2^{N+1}} \left(\begin{array}{l} (\sigma_o + \sigma_z)^{\otimes N} + (\sigma_o - \sigma_z)^{\otimes N} \\ + e^{-N\gamma t} [(\sigma_x + i\sigma_y)^{\otimes N} + (\sigma_x - i\sigma_y)^{\otimes N}] \end{array} \right). \quad (6)$$

Kraus operators of the form $K_1 = \sqrt{p}\sigma_o$ and $K_2 = \sqrt{1-p}\sigma_\alpha$, with $\alpha = x, y, z$, lead to the bit flip, the bit-phase flip, and the phase flip channels, respectively [20].

Of course with the introduction of additional parameters, more general damping models are available, For example, the most general qubit model, subject to constraints that the

decoherence commutes with rotations around the σ_z axis, and is continually differentiable and time stationary, is the model of [21] where $\varepsilon_Z(\rho_s^{GHZ})$

$$= \frac{1}{2^{N+1}} \left(\begin{array}{l} (\sigma_o + [e^{-\gamma_1 t} + \mu(1 - e^{-\gamma_1 t})]\sigma_z)^{\otimes N} \\ + (\sigma_o - [e^{-\gamma_1 t} - \mu(1 - e^{-\gamma_1 t})]\sigma_z)^{\otimes N} \\ + e^{-N(\gamma_2 + i\omega)t} (\sigma_x + i\sigma_y)^{\otimes N} \\ + e^{-N(\gamma_2 - i\omega)t} (\sigma_x - i\sigma_y)^{\otimes N} \end{array} \right), \quad (7)$$

where four real constants γ_1 , γ_2 , μ , and ω are introduced. Some of our previous decoherence models can be seen as special cases of this more general model. For example, setting $\mu = 1$, $\gamma_2 = \gamma_1/2 = \gamma_a/2$, and $\omega = 0$ in Eq. (7) leads to the amplitude damping channel of Eq. (5); and setting $\gamma_2 = \gamma_p$, and $\gamma_1 = \omega = 0$ in Eq. (7) leads to the phase damping channel of Eq. (6).

Combinations of random noise channels and specific damping channels are also possible. For example, consider Kraus operators $K_1 = \sqrt{(1-\varepsilon_1)} \begin{pmatrix} 1 & 0 \\ 0 & \sqrt{1-p} \end{pmatrix}$, $K_2 = \sqrt{(1-\varepsilon_1)} \begin{pmatrix} 0 & \sqrt{p} \\ 0 & 0 \end{pmatrix}$, $K_3 = \sqrt{\varepsilon_3}U_3$, and $K_4 = \sqrt{\varepsilon_4}U_4$, where ε_1 , ε_3 , and ε_4 are in the range $0 - 1$, and where $\varepsilon_1 = \varepsilon_3 + \varepsilon_4$. These operators lead to a quantum channel which approaches amplitude damping as $\varepsilon_1 \rightarrow 0$. In addition, if we let $U_3 = I$ and set $\varepsilon_3 = 1 - e^{-\gamma t}$, for some γ , this allows for a time dependence to be inserted into the additional random component of the channel.

III. RESULTS AND DISCUSSION

We have carried out many simulations over all of the decoherence channels described above for a wide range of parameter settings. Some of these results are shown graphically in Figs. (1)-(4). For the specific random noise channel shown the fidelity given is the average over 10,000 trials. In these plots we have focussed on the high fidelity region, and used cat states for the initial states. For QLV to be functional and unconditional it is important that only states whose fidelities remain high are utilized. A security threat to QLV is the potential ability of an adversary, who is in possession of an optimal cloning machine, copying and redistributing the partial copies of entangled qubits to other devices. If cloning were exact QLV would fail (see [5] for details). However, for optimal cloning F is known to be upper bounded by $F \approx 0.7$ for bipartite entanglement and $F \approx 0.6$ for tripartite entanglement [22], [23]. For a series of two-bit messages encoded in $L = 100$ Bell states, an adversary with access to an optimal cloning machine would have a probability of 1 in 10^{16} of passing the verification system even though not at the authorized location. Arbitrary smaller probabilities are achieved exponentially in L . Within QLV, decoherence must be limited so as to provide for a decoded bit error rate significantly above that expected if an optimal cloning machine was present. Clearly, a value of $F = 0.9$ would suffice in this regard, and we will focus on this value in the discussion of our results.

Our results for the fidelity cannot be directly mapped to true time t , as this would require a detailed understanding

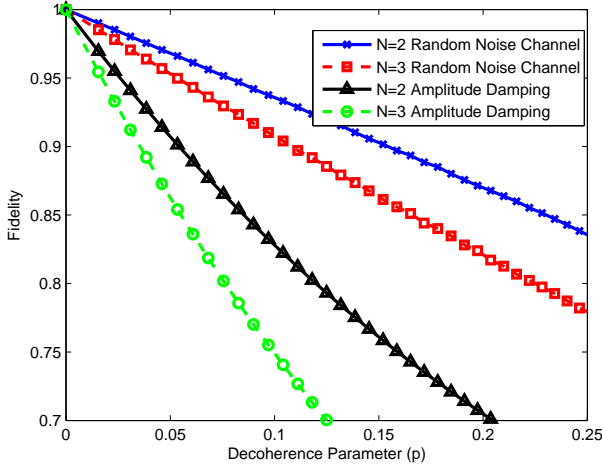


Fig. 1. Fidelity vs. Decoherence Parameter (p) for random noise channels and amplitude damping, for Bell states and $N = 3$ GHZ states.

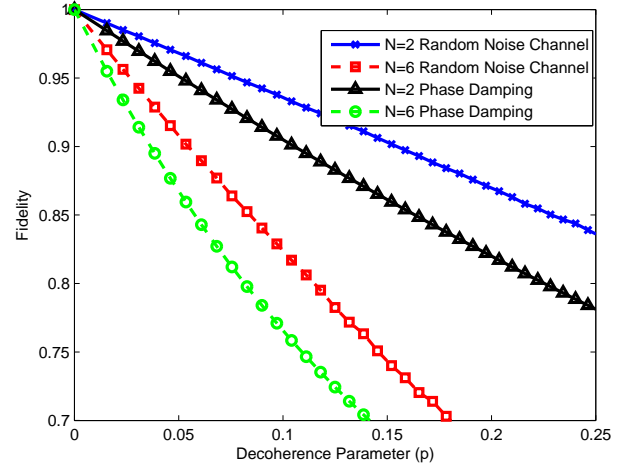


Fig. 3. Fidelity vs. Decoherence Parameter (p), for random noise channels and phase damping, for Bell states and $N = 6$ GHZ states.

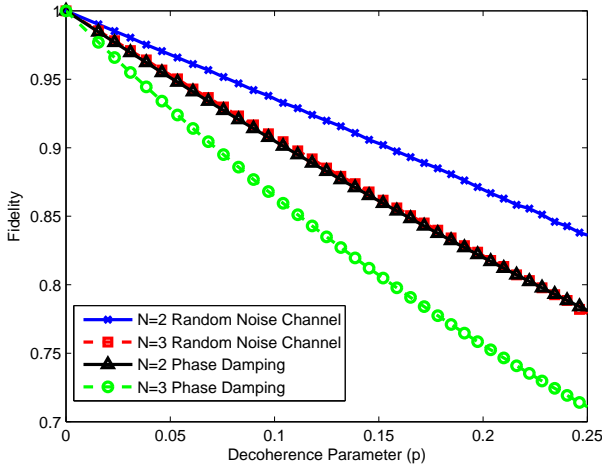


Fig. 2. Fidelity vs. Decoherence Parameter (p), for random noise channels and phase damping, for Bell states and $N = 3$ GHZ states.

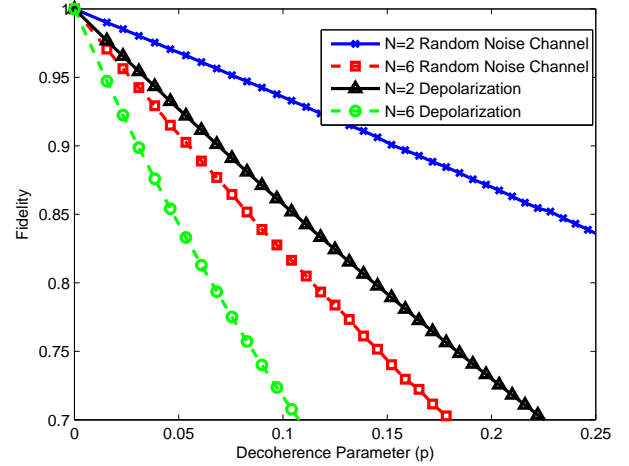


Fig. 4. Fidelity vs. Decoherence Parameter (p), for random noise channels and depolarization, for Bell states and $N = 6$ GHZ states.

of the decoherence rates of the channels. However, they can be used to determine the performance of Bell states relative to N -qubit GHZ states within the QLV context. We can compare performance levels by determining the probability of an instance of location verification. As discussed earlier, an instance of location verification occurs when enough decoding has occurred for a single estimate of location to be obtained. In two dimensional space, timings from at least three reference stations are needed. This means if Bell states are used as the encoding states, then two Bell states must be used in the encoding. If a GHZ state is used, then only one $|\Psi_s^{GHZ}\rangle_{N=3}$ state is required in the encoding. If, following decoherence, F_B and F_{GHZ} are the fidelities of the Bell states and GHZ states, respectively, then the probability of a single instance of location verification for each case can be determined. This is achieved for the Bell state case with probability F_B^2 , whereas

for the GHZ case it would simply be F_{GHZ} .

In Fig. (1) the fidelity as a function of p is shown for the Bell state ($N = 2$ curves) and the $|\Psi_s^{GHZ}\rangle_{N=3}$ state ($N = 3$ curves), in both random noise channels and amplitude damping channels. From this figure we see that a fidelity of $F = 0.9$ is reached at $p \approx 0.07$ for Bell states in the amplitude damping channel. We can also see for the $N = 3$ GHZ state, the fidelity in the amplitude damping channel will be ~ 0.85 at the same p . Recall the probability of a successful instance of location verification for Bell states at $F = 0.9$ will be 0.81. We can see, therefore, that the use of GHZ states will provide slightly better performance relative to Bell states for the specific amplitude damping channel shown. Similar arguments and conclusions also hold with regard to the random noise channels. A similar conclusion to above can be drawn from Fig. (2), where phase damping channels have

been investigated. Again, GHZ states perform slightly better than Bell states for a range of fidelities once the probability of a successful instance of location verification is calculated.

In Fig. (3) the fidelity as a function of p is shown for Bell state ($N = 2$ curves) and the $|\Psi_s^{GHZ}\rangle_{N=6}$ state ($N = 6$ curves) in both random noise channels and phase damping channels. Here we start to see the impact of the faster decoherence of higher dimensional entangled states. In this case, we are modeling the scenario where six reference stations are utilized in order to obtain an instance of location verification. Additional reference stations would increase the location accuracy of the verification. Note, we mean here by increased location accuracy, that achieved by increases in signal-to-noise, and improved dilution of precision effects arising from extra reference stations.³

Fig. (3) is useful for a discussion of the case when we have three Bell states deployed for each instance of location verification. This can be compared to a single decoding of the $|\Psi_s^{GHZ}\rangle_{N=6}$ state. For the Bell states, a target fidelity of 0.9 in the phase damping channel occurs at $p \sim 0.1$. The probability of decoding all three Bell states at this p is then ~ 0.73 . This is approximately the same probability of 0.75 for decoding the $|\Psi_s^{GHZ}\rangle_{N=6}$ state at the same p . This suggests $N = 6$ is close to the limit where higher dimensional states will retain a performance in QLV similar to that achieved with Bell states. Note, however, for Bell states we would need only 2 out of the 3 Bell states to be successfully decoded in order to obtain an instance of location verification. At a target fidelity of 0.9 the probability of this outcome would be 0.97, so in this sense Bell states are operating more efficiently than $|\Psi_s^{GHZ}\rangle_{N=6}$ states. But the removal of one of the Bell states in the decoding would lead to a reduced location accuracy relative to 3 out of 3 Bell state decodings. As such, strictly speaking we should state that the performance (at high fidelity) of the Bell states and $|\Psi_s^{GHZ}\rangle_{N=6}$ states is the same for an instance of location verification at *equal location accuracies*.

In Fig. (4) we can again compare to single decoding of the $|\Psi_s^{GHZ}\rangle_{N=6}$ state to three decodings of Bell states, this time for the depolarization channel of Eq. (4). The results shown in Fig. (4) lead us to a similar conclusion to that drawn previously. That is, generally speaking, there is no significant performance degradation in QLV when a single GHZ state (with $N < 6$) is used in place of multiple Bell states. Although not shown, the constrained σ_z -rotation decoherence of Eq. (7), and damping channels combined with random noise contributions, all lead to a similar general conclusion.

IV. ENTANGLEMENT-SWAPPING QLV

In [5], physical transfer of the qubits is undertaken. Here we introduce a variation to the protocol of [5] where physical transfer of qubits is replaced by teleportation of the qubits.

³Quantum meteorology effects (e.g. [24] [21]) can also provide increased location *accuracy*. However, the additional accuracy obtained via quantum meteorology can also be obtained using additional classical resources (*i.e.* without quantum entanglement). Unconditional location *verification* cannot be achieved using accuracy improvements offered by quantum meteorology, nor can it be achieved with the use of additional classical resources (*i.e.* verification requires quantum entanglement).

The physical transfer is negated by having the device (whose location is to be verified) possess stored qubits that are *a priori* entangled with one reference station.⁴ The ‘trade-off’ is the requirement in the new protocol for quantum memory which can hold state information for much longer timescales relative to the protocol of [5]. This trade-off between physical transfer of qubits and quantum memory requirements, will be of value as advances in quantum memory develop. For clarity we will present the new protocol for a one dimensional location verification using Bell states in which only two reference stations are used. Extensions to the two dimensional problem (three reference stations) are then discussed.

Consider two reference stations at publicly known locations, and a device (Cliff) that is to be verified at a publicly known location (x_v, y_v) . We assume that the reference stations (Alice and Bob) are authenticated and share secure communication channels between each other via quantum key distribution [25], [26]. We also assume that all classical communications between Cliff and the reference stations occur at the speed of light, c . Processing time (*e.g.* due to local quantum measurements) is assumed negligible. Given these assumptions, we wish to unconditionally verify Cliff is at the location (x_v, y_v) .

In QLV a geometrical constraint on the reference stations is always required. For one-dimensional location verification the constraint is that $\tau_{AC} + \tau_{BC} = \tau_{AB}$, where τ_{AC} (τ_{BC}) is the light travel time between Alice (Bob) and Cliff, and where τ_{AB} is the light travel time between Alice and Bob. Let Alice share with Cliff a set of L entangled qubit pairs (*i.e.* a set of L Bell states) $\Omega_i [AC]$, where the subscript $i = 1 \dots L$ labels the entangled pairs. We let the pairs be labeled (*e.g.* by memory address) in the order received from some source, with the first qubit of each pair being held by Alice and the second by Cliff. We will assume an encoding $(00 \rightarrow \frac{1}{\sqrt{2}}(|00\rangle + |11\rangle))$ *etc.* that is public. Let Alice also share with Bob a different set of $L/2$ entangled qubit pairs $\Lambda_j [AB]$, $j = 1 \dots L/2$. Without loss of generality we can assume all entangled qubit pairs are initially in the state $\frac{1}{\sqrt{2}}(|00\rangle + |11\rangle)$. An entanglement-swapping QLV protocol proceeds as follows.

Step 1: Alice initiates an entanglement swapping procedure in order to form a new set $\Gamma_j [BC]$ of $L/2$ entangled pairs between Bob and Cliff. She achieves this by *randomly selecting* one of her local qubits from the pairs $\Omega_i [AC]$, combining this with one of her local qubits sequentially chosen from the pairs $\Lambda_j [AB]$, and conducting a Bell State Measurement (BSM) on the two qubits. These qubits are not selected again for BSM. Alice repeats this process until all of her local qubits from the pairs $\Lambda_j [AB]$ have undergone BSM. At this point Bob shares a new set $\Gamma_j [BC]$ of $L/2$ entangled pairs with Cliff, and Alice shares a reduced set $\Omega_{j'} [AC]$ of $L/2$ entangled pairs with Cliff ($j' = 1 \dots L/2$). We label our sets with the different subscripts i, j, j' to illustrate the following points. Cliff is in possession of L qubits which remain labeled with the index i . He is unaware which reference station (Alice or Bob) each of the qubits in his possession is entangled with.

⁴Such *a priori* entanglement does not by itself produce location authentication since such entanglement can be re-distributed. Note also, the *a priori* entanglement could be used for remote state preparation.

Step 2: Alice communicates with Bob via their secured channel, and informs him of two facts related to each of the local qubits he possesses from the pairs $\Gamma_j [BC]$. Bob is informed of the BSM result relevant to each qubit, and the $j \rightarrow i$ mapping.

Step 3: Alice generates a random binary sequence S_a of length K bits ($K < L$), and shares this sequence with Bob. This sequence is encoded into a different set of Bell states $\Lambda'_j [AB]$ *a priori* shared by Alice and Bob. Who undertakes the local unitary operation needed to encode each two-bit segment of the sequence S_a into $\Lambda'_j [AB]$ is decided by Alice and Bob for each segment.

Step 4: Using a qubit, say qubit j' , from the set $\Omega_{j'} [AC]$, Alice undertakes a BSM with the first qubit she holds from the set $\Lambda'_j [AB]$. Using a classical channel she informs Cliff the outcome of the BSM and the label i of the qubit held by Cliff to which the BSM outcome relates to. This completes the teleportation of the qubit $\Lambda'_1 [AB]$ from Alice to Cliff. Likewise, Bob teleports the corresponding qubit of $\Lambda'_1 [AB]$ held locally by him. The classical messages from Alice and Bob related to the teleportation are sent so as to arrive at the location (x_v, y_v) simultaneously.

Step 5: Using the classical information received from Alice and Bob, Cliff performs a BSM in order to decode two bits of information. Cliff then *immediately* communicates classically to Alice and Bob informing them of the two bits he decoded.

Step 6: Alice checks that the sequence returned to her by Cliff is correctly decoded and notes the round-trip time for the process. Likewise Bob. Alice and Bob can then compare their round-trip times to Cliff ($2\tau_{AC}$ and $2\tau_{BC}$) in order to verify consistency with Cliff's publicly reported location (x_v, y_v) .

Extension of the above protocol to two-dimensional verification could be achieved by the introduction of additional Bell states and a third reference station, say Dan. Alice would repeat the procedures with Dan that she undertook with Bob. With such a set-up, teleportation of two Bell states would be required for an instance of location verification. However, another solution is the use of a $|\Psi_s^{GHZ}\rangle_{N=3}$ state. We will not pursue here a detailed exposition of the protocol in this case, except to note the following. At some point in the protocol one qubit from the $|\Psi_s^{GHZ}\rangle_{N=3}$ state would be held at each of three reference stations. The teleportation of the three qubits to Cliff would comprise an instance of location verification.

The relative performance of two Bell states, as compared to a single $|\Psi_s^{GHZ}\rangle_{N=3}$ state, in the entanglement-swapping protocol just discussed, would follow a similar discussion to that given in Section III. However, we do note the additional entanglement (needed for teleportation) required in the entanglement-swapping protocol would also suffer decoherence. Although this extra decoherence will not directly impact the relative performance of Bell states as compared to a $|\Psi_s^{GHZ}\rangle_{N=3}$ state, it will directly degrade (albeit slightly) the performance of the entanglement-swapping protocol relative to protocols that use direct transfer of qubits.

V. CONCLUSIONS

We have investigated the relative impact of decoherence on QLV protocols. We find that, in general, it is possible to

verify locations using multipartite GHZ states, at a comparable performance level to that obtained using multiple Bell states. Efforts at creating on-demand long-term quantum memory are now bearing fruit, and quantum networks are currently being built and tested. Deployment of QLV protocols in such networks will, for the first time, offer the opportunity to deliver real-time communications systems which can be made unconditionally dependent on the physical location of a receiver.

REFERENCES

- [1] Scott, L. and Denning, D. E., "Geo-Encryption: Using GPS to enhance data security," *GPS World*, April 2003, 40-49 (2003).
- [2] Capkun, S. and Hubaux, J-P., "Secure positioning in wireless networks," *IEEE JSAC*, Vol. 24, 221-232 (2006).
- [3] Malaney, R. A., "Wireless intrusion detection using tracking verification," *IEEE International Conference on Communications (ICC '07)*, Glasgow, 1558-1563 (2007).
- [4] Chiang, J. T., Haas, J. J. and Hu, Y.-C., "Secure and precise location verification using distance bounding and simultaneous multilateration," *WiSec09*, Zurich, Switzerland (2009).
- [5] Malaney, R. A., "Location-dependent communications using quantum entanglement," *Phys. Rev. A* 81, 042319, DOI: 10.1103/PhysRevA.81.042319 (2010).
- [6] Wootters, W. K. and Zurek, W. H., "A single quantum cannot be cloned," *Nature* 299, 802-803 (1982).
- [7] Bennett, C. H. and Wiesner, S. J., "Communication via one- and two-particle operators on Einstein-Podolsky-Rosen states," *Phys. Rev. Lett.* 69, 2881 - 2884 (1992).
- [8] Barreiro, J. T., Wei, T. C. and Kwiat, P. G., "Beating the channel capacity limit for linear photonic superdense coding," *Nature Physics*, Vol.4, 282-286 (2008).
- [9] Bennett, C. H. *et al.*, "Teleporting an unknown quantum state via dual classical and EPR channels," *Phys. Rev. Lett.* 70, 1895-1899 (1993).
- [10] Ursin, R. *et al.*, "Entanglement-based quantum communication over 144km," *Nature Physics* 3, 481-486 (2007).
- [11] Kaltenbaek, R., Prevedel, R., Aspelmeyer, M. and Zeilinger, A., "High-fidelity entanglement swapping with fully independent sources," *Phys. Rev. A* 79, 040302(R) (2009).
- [12] Peev, M. *et al.*, "The SECOQC quantum key distribution network in Vienna. *The New Journal of Physics*," 11, 075001 (2009).
- [13] Simon, C., *et al.*, "Quantum Memories. A Review based on the European Integrated Project Qubit Applications (QAP)," arXiv:1003.1107v1 [quant-ph], (2010).
- [14] Sangouard, N., *et al.*, "Robust and efficient quantum repeaters with atomic ensembles and linear optics," *Phys. Rev. A* 77, 062301 (2008).
- [15] Greenberger, D. M., Horne, M. A. and Zeilinger, A., "Going beyond Bells theorem," in *Bell's Theorem, Quantum Theory, and Conceptions of the Universe*, M. Kafatos (ed.), (Kluwer, Dordrecht) 73-76 (1989).
- [16] Gao, W. B., *et al.*, "Experimental demonstration of a hyper-entangled ten-qubit Schrodinger cat state," *Nature Physics*, doi:10.1038/nphys1603 (2010).
- [17] Kraus, K., "States, Effects and Operations," (Springer-Verlag), (1983).
- [18] Nakakara, M., "Quantum computing: An overview," in *Mathematical Aspects of Quantum Computing*, World Scientific (2007).
- [19] Gregoratti, M. and Werner, R. F., "Quantum Lost and Found," *J. Mod. Opt.* 50, 915 (2003).
- [20] Nielsen, M. A. and Chuang, I. L., *Quantum Computation and Quantum Information*, Cambridge Univ. Press, (2000).
- [21] Shaji, A and Caves, C. M., "Qubit metrology and decoherence," *Phys. Rev. A* 76, 032111 (2007).
- [22] Lamoureaux, L. P., Navez, P., Fiurek, J., and Cerf, N. J., "Cloning the entanglement of a pair of quantum bits," *Phys. Rev. A* 69, 040301R (2004).
- [23] Karpov, E., Navez, P., and Cerf, N. J., "Cloning quantum entanglement in arbitrary dimensions," *Phys. Rev. A* 72, 042314 (2005).
- [24] Giovannetti, V., Lloyd, S., and Maccone, L., "Quantum-enhanced positioning and clock synchronization," *Nature* 412, 417 (2001).
- [25] Bennett, C. H. and Brassard, G., "Public key distribution and coin tossing," *Proc. IEEE Int. Conf. on Computers, Systems and Signal Processing*, Bangalore, India, 175-179 (1984).
- [26] Ekert, A. K., "Quantum cryptography based on Bell's theorem," *Phys. Rev. Lett.* 67, 661-663 (1991).